Supplement of Atmos. Chem. Phys., 20, 4713–4734, 2020
https://doi.org/10.5194/acp-20-4713-2020-supplement

Atmospheric Chemistry and Physics
Open Access
EGU

Supplement of

Influence of vessel characteristics and atmospheric processes on the gas and particle phase of ship emission plumes: in situ measurements in the Mediterranean Sea and around the Arabian Peninsula

Siddika Celik et al.

Correspondence to: Frank Drewnick (frank.drewnick@mpic.de)

S1 Trigonometrical equations for the identification of ship emission plume sources

This section refers to the calculations described in Sect. 2.3 of the main text.

S1.1 Regular case

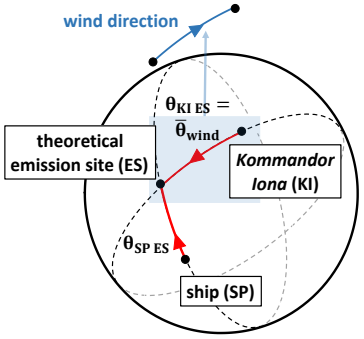

Figure S1: Illustration of the determination of the intersection point(s) of two great circles on a sphere. Two positions (*here*: geographic position of the *Kommandor Iona* (KI) and of the other ship (SP)) as well as the initial bearings starting from these positions (*here*: average wind direction over ground ($\bar{\theta}_{wind}$) and vessel course ($\theta_{SP\ ES}$)) towards the intersection point (*here*: theoretical emission site) have to be given in order to determine the sought intersection point according to Eqs. (S2) to (S12). It has to be mentioned that the bearing between the *Kommador Iona* and the theoretical emission site ($\theta_{KI\ ES}$) equals the angle value of the average wind direction.

1. Calculation of the average wind direction according to directional statistics (Mardia and Jupp, 2000):

$$\bar{\theta}_{wind} = \begin{cases} \arctan\left(\frac{n^{-1}\sum_{i=1}^{n}\sin(\theta_{wind,i})\cdot v_{wind,i}}{n^{-1}\sum_{i=1}^{n}\cos(\theta_{wind,i})\cdot v_{wind,i}}\right), & \text{if denom.} \geq 0 \text{ and num.} \geq 0 \\ -\text{''}- + 2\pi, & \text{if denom.} \geq 0 \text{ and num.} < 0 \\ -\text{''}- + \pi, & \text{if denom.} < 0, \end{cases} \quad \text{(S1)}$$

where θ_{wind} is the wind direction over ground, v_{wind} the wind speed over ground and i the i–th wind data point and n the number of wind data points within the averaging interval.

2. Determination of the theoretical emission site according to nautical equations (Veness, 2019) with all angles in radian; if not otherwise stated, angles describe positions on the globe:
   i. Calculation of the angular distance (δ) between the ship (SP) and the *Kommandor Iona* (KI) positions using the geographic longitudes (LON) and latitudes (LAT) of both positions:

$$x = \sin^2\left[\frac{LAT_{KI} - LAT_{SP}}{2}\right] + \cos(LAT_{SP}) \cdot \cos(LAT_{KI}) \cdot \sin^2\left[\frac{LON_{KI} - LON_{SP}}{2}\right], \quad \text{(S2)}$$

$$\delta_{SP\ KI} = 2\arcsin\left[\sqrt{x}\right]. \quad \text{(S3)}$$

ii. Calculation of the bearing (θ) between the ship and the *Kommandor Iona* as well as between the *Kommandor Iona* and the ship using the geographic longitudes and latitudes of both positions and the angular distance given in Eq. (S2) and (S3):

$$\boldsymbol{\theta_a = \arccos\left[\frac{\sin(LAT_{KI}) - \sin(LAT_{SP})\cdot\cos(\delta_{SP\,KI})}{\sin(\delta_{SP\,KI})\cdot\cos(LAT_{SP})}\right]}, \tag{S4}$$

$$\boldsymbol{\theta_b = \arccos\left[\frac{\sin(LAT_{SP}) - \sin(LAT_{KI})\cdot\cos(\delta_{SP\,KI})}{\sin(\delta_{SP\,KI})\cdot\cos(LAT_{KI})}\right]}, \tag{S5}$$

$$\left.\begin{aligned}\boldsymbol{\theta_{SP\,KI}} &= \boldsymbol{\theta_a}\\ \boldsymbol{\theta_{KI\,SP}} &= \boldsymbol{2\pi - \theta_b}\end{aligned}\right\}\ \textbf{if}\ \boldsymbol{\sin(LON_{KI} - LON_{SP}) > 0}$$
$$\left.\begin{aligned}\boldsymbol{\theta_{SP\,KI}} &= \boldsymbol{2\pi - \theta_a}\\ \boldsymbol{\theta_{KI\,SP}} &= \boldsymbol{\theta_b}\end{aligned}\right\}\ \textbf{else}. \tag{S6}$$

iii. Calculation of the angles (α) of the triangle spanned by the position of the ship, the position of the *Kommandor Iona* and the theoretical emission site (ES). The angle at the position of the ship (α_{SP}; or at the *Kommandor Iona* (α_{KI})) is calculated using the bearing which is given in Eqs. (S4) and (S6) (or in Eqs. (S5) and (S6)) and the vessel course ($\theta_{SP\,ES}$; or the average wind direction). The angle at the theoretical emission site (α_{ES}) is calculated using the angles at the position of the ship and at the *Kommandor Iona* as well as the angular distance given in Eqs. (S2) and (S3):

$$\boldsymbol{\alpha_{SP} = \theta_{SP\,ES} - \theta_{SP\,KI}}, \tag{S7}$$

$$\boldsymbol{\alpha_{KI} = \theta_{KI\,SP} - \overline{\theta}_{wind}}, \tag{S8}$$

$$\boldsymbol{\alpha_{ES} = \arccos[-\cos(\alpha_{SP})\cdot\cos(\alpha_{KI}) + \sin(\alpha_{SP})\cdot\sin(\alpha_{KI})\cdot\cos(\delta_{SP\,KI})]}. \tag{S9}$$

iv. Calculation of the angular distance between the ship position and the theoretical emission site using the angles given in Eqs. (S7) to (S9) as well as the angular distance given in Eqs. (S2) and (S3):

$$\boldsymbol{\delta_{SP\,ES} = \operatorname{arctan2}[\sin(\delta_{SP\,KI})\cdot\sin(\alpha_{SP})\cdot\sin(\alpha_{KI}), \cos(\alpha_{KI}) + \cos(\alpha_{SP})\cdot\cos(\alpha_{ES})]}. \tag{S10}$$

v. Calculation of the position of the theoretical emission site using the geographic latitude of the ship position, using the vessel course and using the angular distance given in Eq. (S10):

$$\boldsymbol{LAT_{ES} = \arcsin[\sin(LAT_{SP})\cdot\cos(\delta_{SP\,ES}) + \cos(LAT_{SP})\cdot\sin(\delta_{SP\,ES})\cdot\cos(\theta_{SP\,ES})]}, \tag{S11}$$

$$\boldsymbol{LON_{ES} = LON_{SP} + \operatorname{arctan2}[\sin(\theta_{SP\,ES})\cdot\sin(\delta_{SP\,ES})\cdot\cos(LAT_{SP}),\ \cos(\delta_{SP\,ES}) - \sin(LAT_{SP})\cdot\sin(LAT_{ES})]}. \tag{S12}$$

3. Calculation of the geographic distance between two positions using the Haversine formula (Veness, 2019):

$$\boldsymbol{d = 2R\cdot\operatorname{arctan2}\left[\sqrt{x}, \sqrt{1-x}\right]}, \tag{S13}$$

where d is the geographic distance between two positions and R the earth radius of 6 371 km (Veness, 2019). x is given in Eq. (S2).

S1.2 Exceptional cases

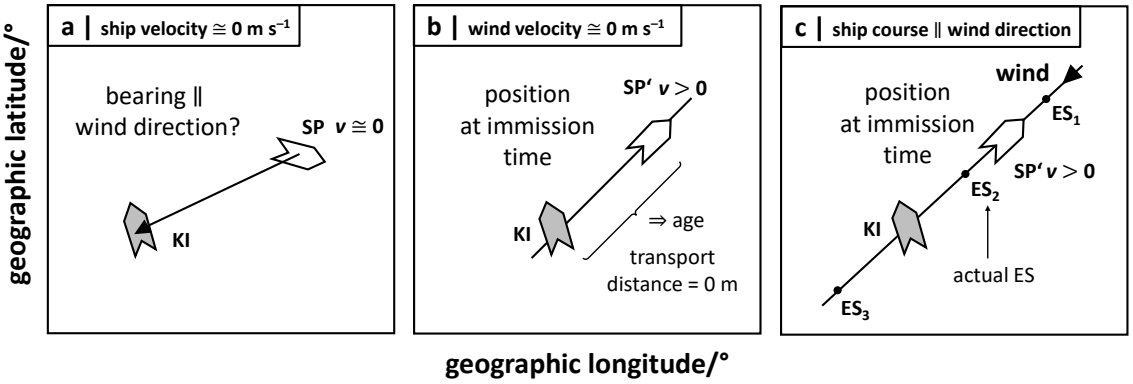

Figure S2: Illustration of exceptional cases of vessel identification. The case of a stationary vessel as emission source (a), the case of wind velocities close to 0 m s^{-1} (b) and the case of a ship with a course that was (anti–)parallel to the wind direction as emission source (c) are presented. KI stands for *Kommandor Iona*, SP for ship and ES for theoretical emission site.

1. In case of a stationary vessel ($v_{\mathrm{ship}} \sim 0$ m s^{-1}) as emission source the average wind direction was parallel to the bearing starting from the vessel towards the measurement location (see Fig. S2 (a)), whereas the bearing was calculated in analogy to Eqs. (S4) and (S6).
2. In case of low wind velocities ($v_{\mathrm{wind}} \sim 0$ m s^{-1}) we expect the emission plume to have been spread along the vessel track as the wind did not significantly transport the plume. In case the *Kommandor Iona* crossed the other vessel's track at the measurement time under low wind velocity conditions (see Fig. S2 (b)) (visual decision), the listed steps were followed:
    i. Determination of the time difference between the measurement time and time of the AIS record. The time difference is considered positive for an AIS record earlier than the measurement time and otherwise negative.
    ii. Calculation of the distance the vessel covers during the time given in 2.i. using the vessel speed. The distance is considered negative for a negative and positive for a positive time difference.
    iii. Calculation of the ship position at the measurement time by analogy to Eqs. (S11) and (S12) using the AIS position, the absolute value of the distance given in 2.ii. (the angular distance equals the ratio between the distance and the earth radius) and the ship course in case of a positive distance (the anti-parallel ship course in case of a negative distance).
    iv. The considered vessel caused the measured ship emission event, if it was at the measurement location before the *Kommandor Iona*, which is true if the vessel course is parallel to the bearing starting from the measurement site towards the ship position at the measurement time. The bearing was calculated in analogy to Eqs. (S4) and (S6).

3. In case of (anti–)parallel wind direction and vessel course and the *Kommandor Iona* crossing the other vessel's track at the measurement time (see Fig. S2 (c)) (visual decision) the listed steps were followed:

   i. Calculation of the position at the measurement time in analogy to steps 2.i. to 2.iii.

   ii. Calculation of the distance between the measurement site and the ship position at the measurement time ($\overline{\mathrm{KI\ SP'}}$) in analogy to Eqs. (S2) and (S13). The emission site equals one of the following three, if the conditions are fulfilled.

   iii. The emission site was between both vessel positions (see ES_2 in Fig. S2 (c)), if the other ship was upwind as well as if the wind direction and ship course were antiparallel because the emission occurred earlier than its detection. Considering that the wind requires the same time (t) to travel the distance between the emission site and the *Kommandor Iona* ($\overline{\mathrm{KI\ ES}}$) as the ship needs to cover the distance between the emission site and the ship position at the measurement time ($\overline{\mathrm{ES\ SP'}}$), the unknown distance $\overline{\mathrm{KI\ ES}}$ was calculated according to Eqs. (S14) and (S15) using the ship (v_{ship}) and the average wind velocity ($\bar{v}_{\mathrm{wind}}$).

$$\boldsymbol{t = \overline{KI\ ES}/\bar{v}_{wind}}, \tag{S14}$$

$$\boldsymbol{\overline{KI\ SP'} = \overline{KI\ ES_2} + \overline{ES_2\ SP'} = (\bar{v}_{wind} + v_{ship}) \cdot t} \tag{S15}$$

   iv. The emission site was beyond the other vessel (see ES_1 in Fig. S2 (c)), if the ship course and wind direction were parallel and directed towards the *Kommandor Iona* and if the wind velocity was higher than the ship velocity. Calculations followed Eqs. (S14) and (S16).

$$\boldsymbol{\overline{KI\ SP'} = \overline{KI\ ES_1} - \overline{ES_1\ SP'} = (\bar{v}_{wind} - v_{ship}) \cdot t} \tag{S16}$$

   v. The emission site was beyond the *Kommandor Iona* (see ES_3 in Fig. S2 (c)), if the ship course and wind direction were parallel and directed away from the *Kommandor Iona* and if the wind velocity was lower than the ship velocity. Calculations followed Eq. (S14) and (S17).

$$\boldsymbol{\overline{KI\ SP'} = \overline{ES_3\ SP'} - \overline{KI\ ES_3} = (v_{ship} - \bar{v}_{wind}) \cdot t} \tag{S17}$$

S2 Additional graphics from analysis

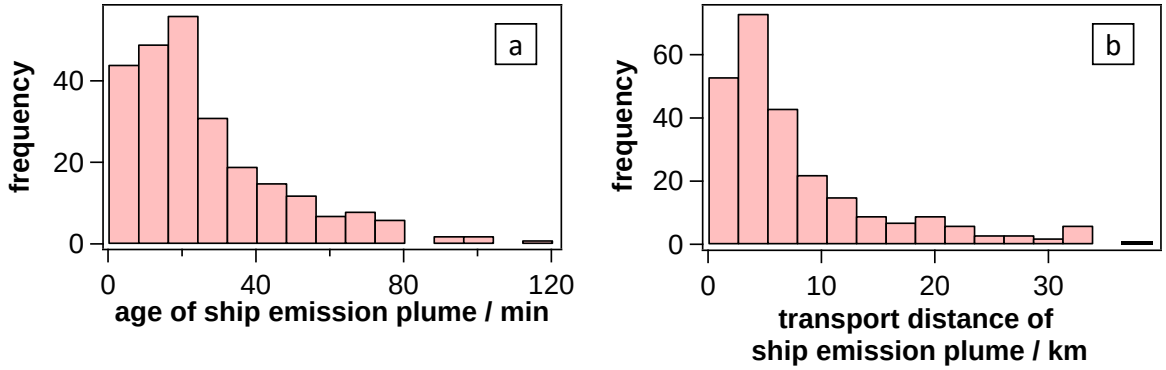

Figure S3: Frequency distributions of the age (a) and transport distance (b) of 252 identified ship emission events in the AQABA dataset. The bins are equidistant with 8 min for (a) and ~ 2.5 km for (b).

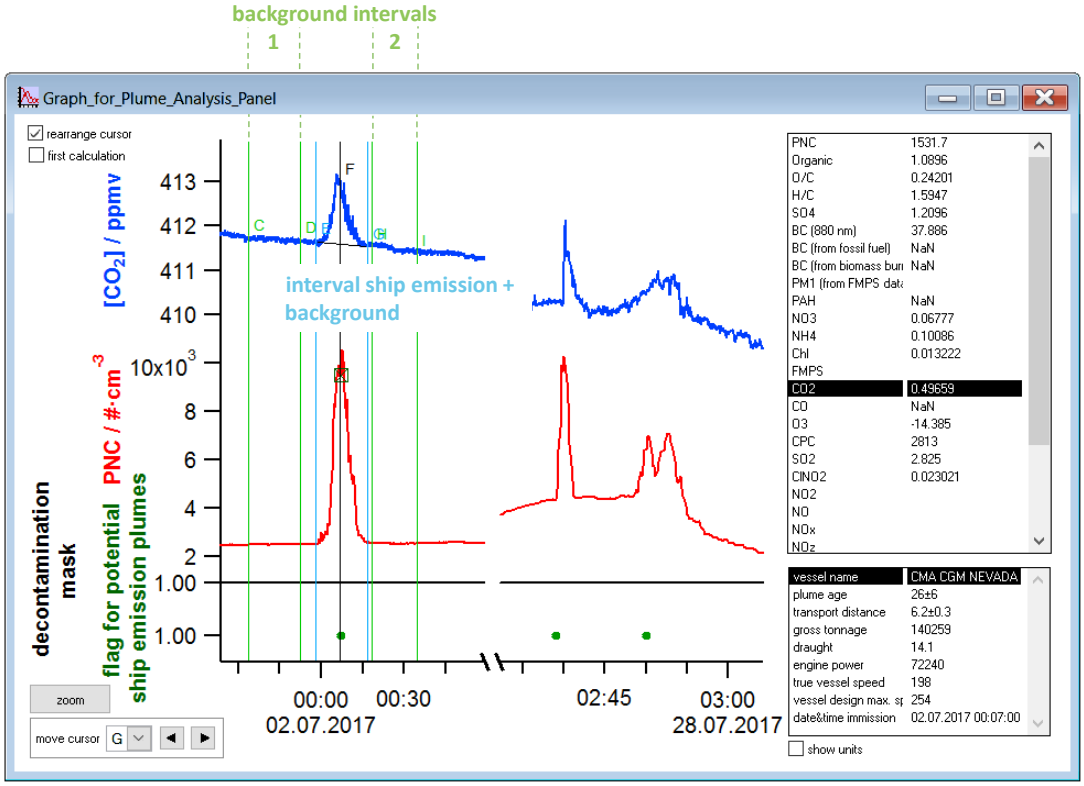

Figure S4: Graphical output of the software for the calculation of quantities of ship emission events that were identified in the AQABA dataset. Example events as well as limits set for the background intervals and those set for the interval including the ship emission event are displayed.

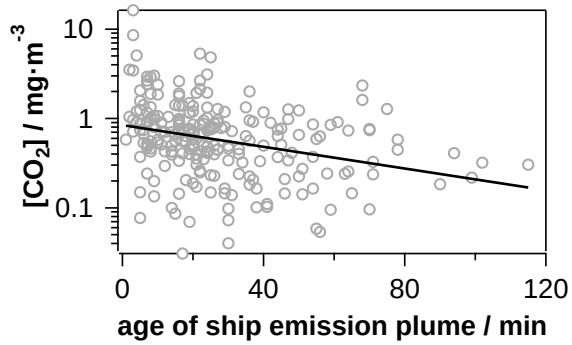

Figure S5: Atmospheric dilution of ship emission plumes. Average excess CO_2 plume concentrations (rel. uncertainty (combined rel. quantification and measurement uncertainties): 5 %) are displayed against the plume age (avg. rel. uncertainty: 20 %). The linear fit of logarithmic time dependent average excess CO_2 concentrations ($N = 252$) follows $\ln([CO_2][\text{mg m}^{-3}]) = -0.14 - 0.014 \cdot t[\text{min}]$ with Pearson's $R = 0.30$. The dispersion lifetime of CO_2 (given as e–folding time) in the ship emission plume is given by the absolute value of the reciprocal regression slope and equals (70 ± 15) min.

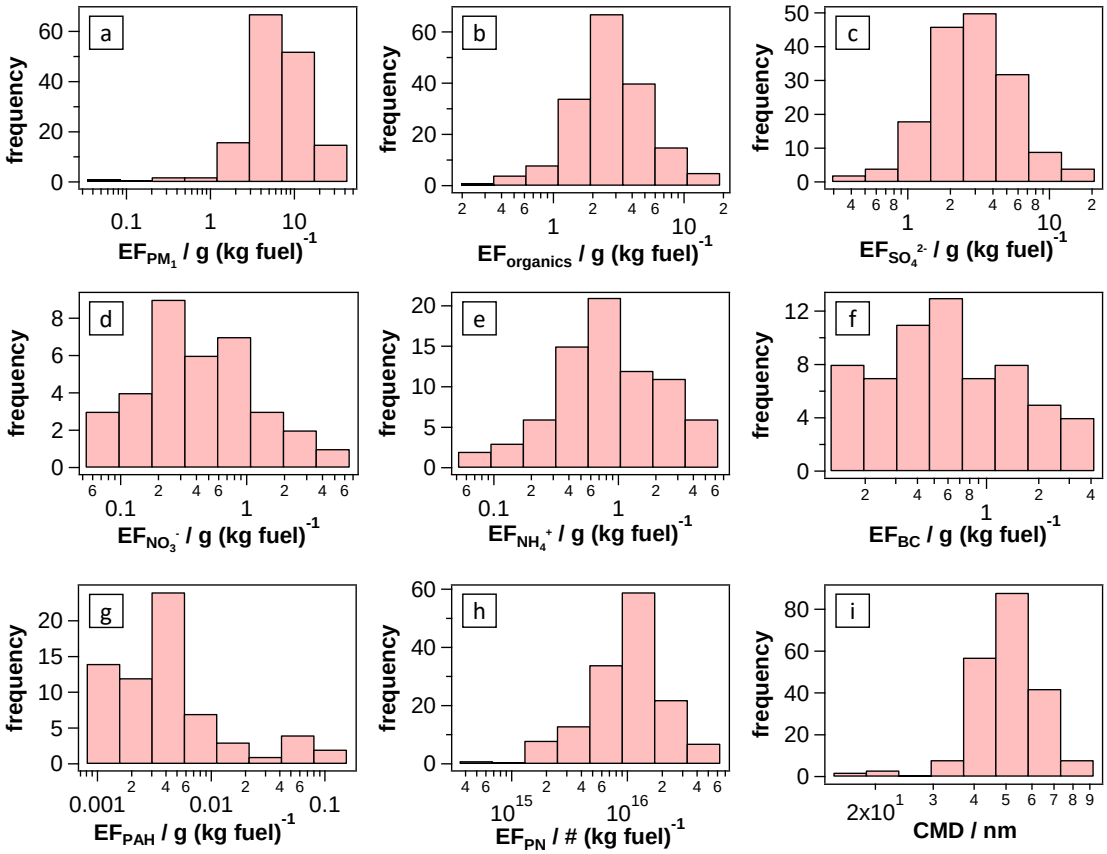

Figure S6: To be continued.

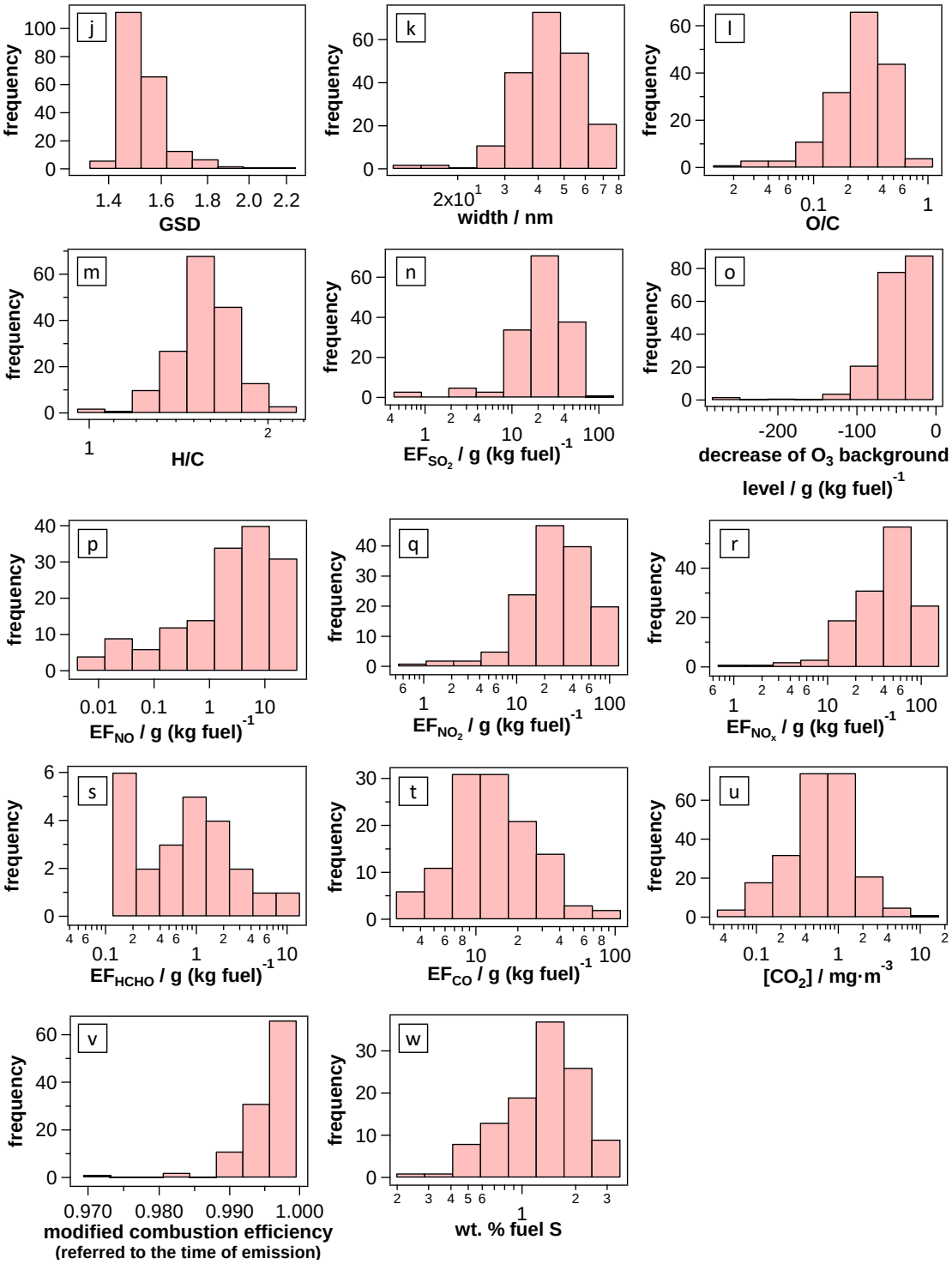

Figure S6: Frequency distributions of calculated plume quantities of identified ship emission events in the AQABA dataset. The bins are equidistant on logarithmic scale, except in case of panel (o), where the bins are equidistant on linear scale.

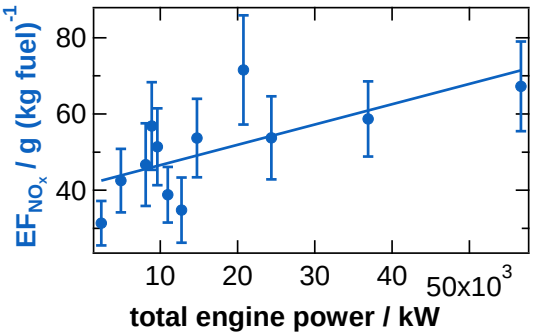

Figure S7: Dependency of the NO_x emission factor on the total vessel engine power P as provided from the AIS data base for the individual ships. Error bars present the combination of estimated quantification and measurement uncertainties and one sigma standard deviations of the data distributions in each bin. The linear fit of the binned data ($N = 140$) follows EF_{NO_x}[g (kg fuel)$^{-1}$] = 41+5.3·10^{-4}·P[kW] with Pearson's $R = 0.30$.

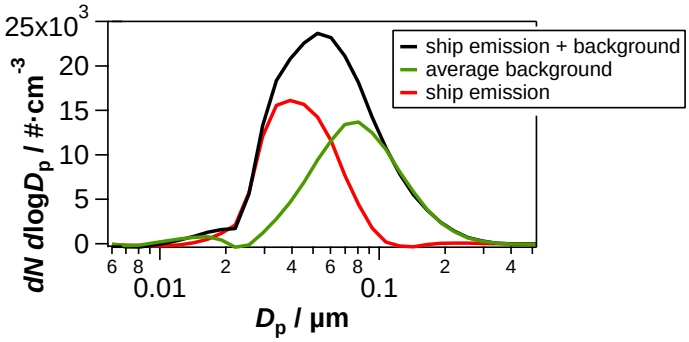

Figure S8: Illustration of the determination of a ship emission plume's particle size distribution based on an example event. For this purpose, the average particle number size distribution of the background was subtracted from the average particle number size distribution measured during the event.

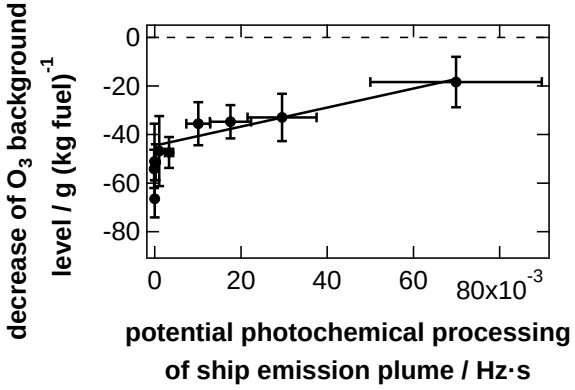

Figure S9: Initial O_3 depletion caused by excess NO in ship emission plumes and the photochemical recovery over time. The linear fit of the binned data ($N = 202$) follows O_3–loss[g (kg fuel)$^{-1}$] = −45+392·JO^{1}D·t[Hz·s] with Pearson's $R = 0.17$.

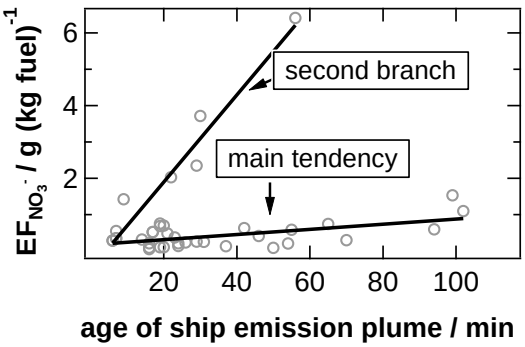

Figure S10: Dependency of the NO_3^- emission factor (rel. uncertainty: 36 %) on the age of the ship emission plume (avg. rel. uncertainty: 20 %). The linear fit follows either $EF_{NO_3^-}$[g (kg fuel)$^{-1}$] = 0.17 + 0.0070·t[min] with Pearson's $R = 0.58$ (main tendency; $N = 31$) or $EF_{NO_3^-}$[g (kg fuel)$^{-1}$] = 0.12·t[min] with Pearson's $R = 0.96$ (second branch; $N = 8$).

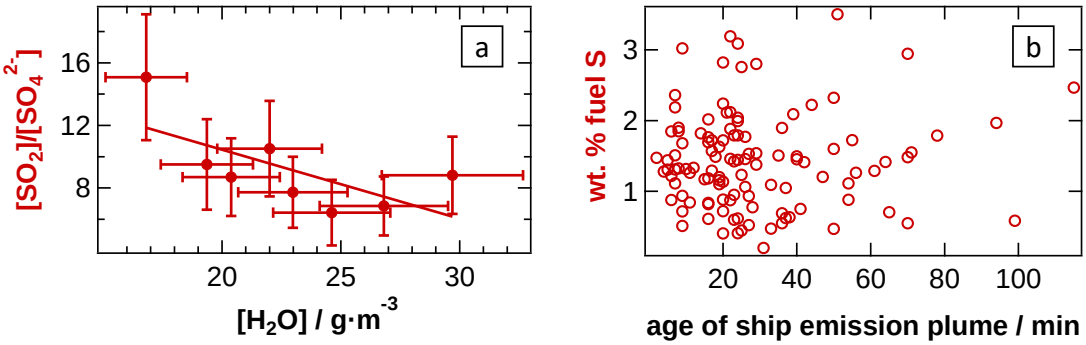

Figure S11: Dependency of the SO_2 to SO_4^{2-} ratio of average excess concentrations on the water vapor concentration, i.e. the absolute humidity (a), and the independency of the weight percentage of fuel sulfur (rel. uncertainty: 42 %) on the age of the ship emission plume (avg. rel. uncertainty: 20 %) (b). The linear fit of the binned data in (a) follows $[SO_2]/[SO_4^{2-}] = 19 - 0.44 \cdot [H_2O]$[g m^{-3}] with Pearson's $R = 0.21$. Panel (a) includes 125 data points and panel (b) 114.

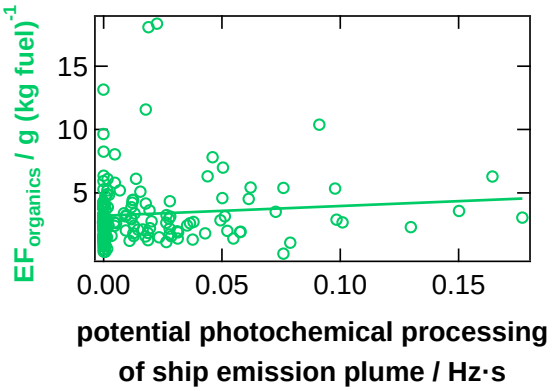

Figure S12: Dependency of the particulate organic emission factor (rel. uncertainty: 37 %) on the potential photochemical processing of a ship emission plume (avg. rel. uncertainty: 27 %). The linear fit of the data (N = 174) follows $EF_{organics}$[g (kg fuel)$^{-1}$] = 3.2+7.6·JO^{1}D·t[Hz·s] with Pearson's R = 0.06.

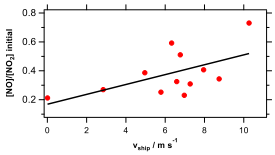

Figure S13: Dependency of the calculated initial (i.e. for the point of emission) NO to NO_2 ratio (av. rel. uncertainty: 40 %) on the vessel speed. The linear fit of the data (N = 157) follows [NO]/[NO_2] = 0.179+0.032·v_{ship}[m·s^{-1}] with Pearson's R = 0.34.

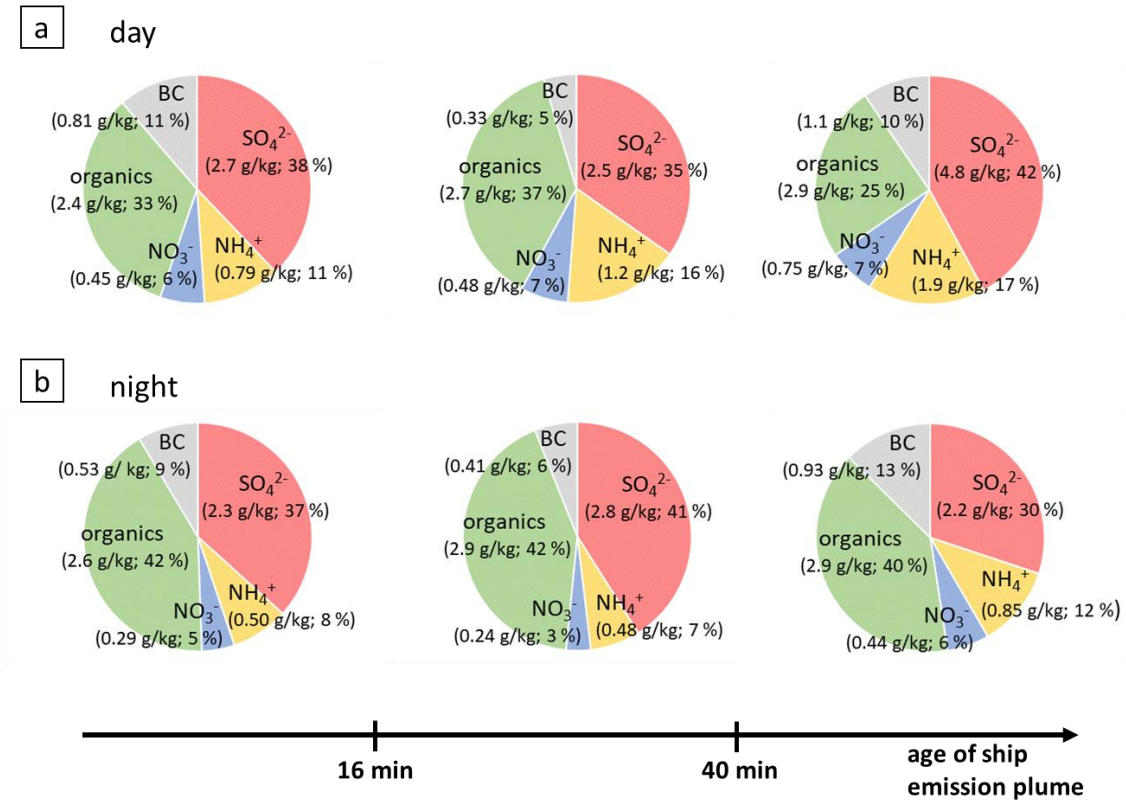

Figure S14: The typical chemical composition (calculated from median EFs) of the particle phase is presented for ship emission plumes younger than 16 min, between 16 min and 40 min of age, and older than 40 min, separated for plumes observed during the day (a) and during night time (b).

References

Mardia, K. V., and Jupp, P. E.: Directional statistics, Wiley, Chichester, UK, 2000.

Veness, C.: Movable Type Scripts: Calculate distance, bearing and more between Latitude/Longitude points, Movable Type Ltd, https://www.movable-type.co.uk/scripts/latlong.html, 2019.